Dimensioning method for precharged membrane expansion vessels for pressure maintenance of hydronic systems

Ralph Eismann
Institute of Sustainability and Energy in Construction, University of Applied Science North-Western Switzerland FHNW; Hofackerstrasse 30, CH-4132 Muttenz, Switzerland
Correspondence: ralph.eismann@fhnw.ch; Tel.: +41 61 228 53 61

Abstract: Effective pressure maintenance is essential to ensure fault-free and energy-efficient operation of hydronic systems. Precharged membrane expansion vessels (MEV) are widely used for this purpose. A membrane within these MEVs separates the liquid connected to the circuit from the fixed amount of gas. Several standards provide dimensioning methods. However, these methods have two main disadvantages. First, pressure measurement uncertainties are not considered. Second, changes in the MEV temperature are neglected. The resulting uncertainties in dimensioning, commissioning, and maintenance can lead to malfunction and damage.

Based on the extremal states of both the circuit and the MEV, an improved and generalized dimensioning method was derived. The change in the gas temperature within the MEV is accounted for. The measurement uncertainties of preset- and system-pressure, as well as average MEV and circuit temperature, are considered. Furthermore, this method accounts for temporary process volumes that can occur, for example, during vacuum degassing or the stagnation of solar thermal circuits. By applying the new method, operational failures owing to incorrectly dimensioned MEVs, or faulty maintenance can be avoided. For simple commissioning and maintenance, corresponding software is provided as a free, open-source tool.

Keywords: Hydronic circuit, Pressure maintenance; Membrane expansion vessel; Expansion tank; Operational safety.

1. Introduction

Pressure maintenance has rarely been the subject of scientific discussions in peer-reviewed journals. Therefore, it is necessary to explain the purpose and applications of pressure maintenance in general (Section 1.1), followed by a definition of pressure maintenance using membrane expansion vessels (MEVs) (Section 1.2). The methods, assumptions, and definitions of the dimensioning methods are discussed in Section 1.3. After this preparation, the available literature on MEV dimensioning is discussed in Section 1.4. In Section 1.5, the goals of this work are formulated: the derivation of a generalized dimensioning method for MEVs, which follows in Chapter 2.
This study is limited to theoretical derivations as in prior studies.

1.1. Pressure maintenance – purpose and applications

Hydronic systems, such as heating networks, cooling circuits, and solar thermal circuits are equipped with pressure-maintenance systems (PMS). The two main components of a PMS are the expansion vessel (also referred to as the expansion tank or expansion chamber), which enables thermal-volume changes in the heat carrier, and the safety valve. The primary purpose of a PMS is to maintain the system pressure within well-defined limits. The upper limit is determined using a safety valve. The lower limit is set such that the pump-inlet pressure is sufficiently high and the pressure, at any point in the circuit, does not fall below the vapor pressure or atmospheric pressure. An additional purpose of PMS is to compensate small liquid losses. The PMS must function correctly for the trouble-free, energy-efficient operation of a hydronic system. Figure 1 shows different types and modes of operation of PMS expansion vessels.

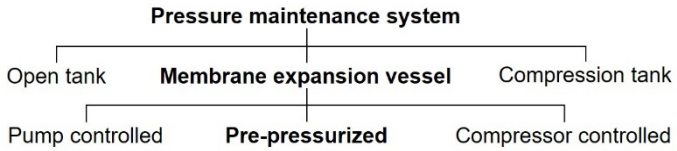

Figure 1. Different types of PMS.

A PMS with an open tank has a free liquid/air interface and is open to the atmosphere. The tank is placed above the circuit highpoint, so that the desired overpressure within the circuit was/is created by the hydrostatic pressure of the liquid column.

A PMS based on a closed expansion tank has also a free liquid/gas interface. The tank is pressurized using compressed air or nitrogen (ASHRAE 2020).

Since their invention, by Stuecklin (1959) and Kirk (1962), MEVs have revolutionized the pressure maintenance of hydronic systems. An MEV consists of a steel vessel and membrane. The membrane separates the gas from the liquid content and thus prevents gas from being absorbed by the liquid. Owing to this feature, MEVs can be located at any point in the circuit. Furthermore, the gas content of the circuit can be substantially reduced by degassing, without affecting the function of the MEV. This paper focuses on MEVs with a fixed gas content, whose design and function are described in the following section. Compressor- and pump controlled MEVs (VDI 4708-1 2012) are not discussed.

1.2. Pressure maintenance using precharged MEVs

There are two major classes of MEV designs, as shown in Figure 2. In MEVs with diaphragm-type membranes, the rim of the membrane is attached to the inner circumference of the vessel, and the liquid content of the MEV is in contact with the wall. In MEVs with bladder-type membranes, the liquid is usually contained within the bladder. A gas valve enables precharging prior to

commissioning the circuit. The liquid side of the MEV is connected to the circuit via an expansion line.

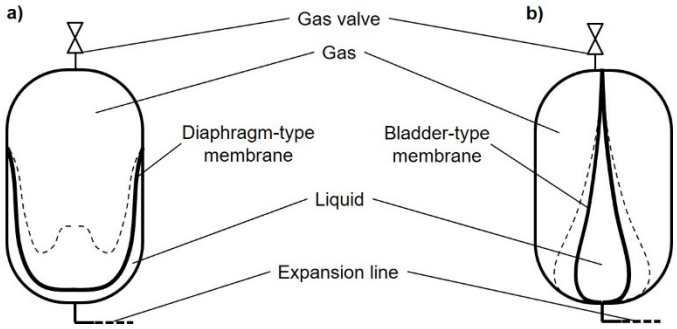

Figure 2. Membrane expansion vessel a) with diaphragm-type membrane, and b) with bladder-type membrane.

Figure 3a) shows an MEV where the gas occupies the entire nominal volume, V_N, and the preset pressure is p_0.

Figure 3b) shows an MEV connected to a heating or cooling circuit. For pressure to be transferred from the gas to the circuit, a liquid volume must always be present within the MEV. Therefore, the preset pressure must be lower than the liquid pressure within the circuit at the reference level, h_0. Any volumetric liquid transfer between circuit and MEV leads to a reverse change in gas volume of equal magnitude inside the MEV. The location at which the expansion line connects to the circuit is called the integration point. If required, an MEV can be thermally decoupled from the circuit by an intermediate vessel (IV).

Figure 3c) shows an MEV connected to a solar thermal circuit. Stagnation produces a large volume of vapor. The corresponding volume of liquid must be displaced into the MEV. To protect the pump from hot liquid, and to allow displacement via the supply and return lines, the reference point must be on the pressure-side of the pump, and downstream of the check valve (CV).

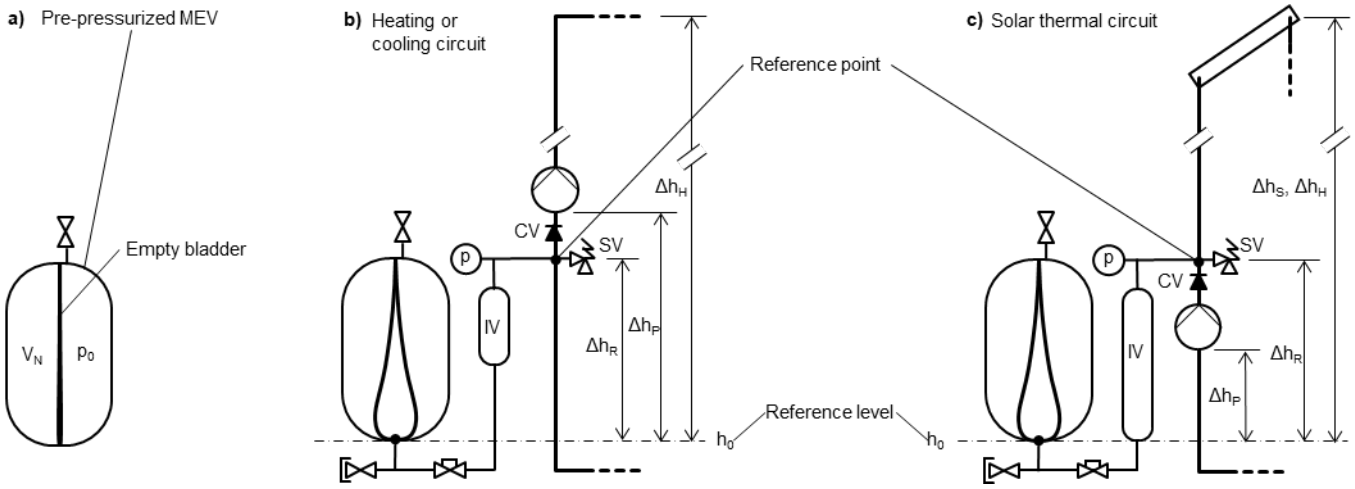

Figure 3. a) Precharged MEV, b) MEV connected to a heating or cooling circuit,
c) MEV connected to a solar thermal circuit.

1.3. Methods, definitions, and assumptions

To facilitate comparison of methods, a unified notation of the state variables and indices is used, as listed in Appendix A.

Dimensioning of MEVs is based on the transition between clearly defined states $k \in \{0,1,2,3\}$, using the ideal gas model, $pV/T = \text{const}$. State 0 indicates the state of the precharged MEV. Additionally, State *F* indicates an arbitrary filling state that occurs at commissioning or maintenance.

It is assumed that volume changes result in shape changes of the membrane rather than stretching. Consequently, the pressure difference across the membrane is negligible.

In the absence of reliable data, and for the sake of simplicity, it is assumed that the liquid pressure at the reference level equals the gas pressure inside the MEV.

The spring-loaded check valve suppresses circulation due to density differences when the pump is switched off. Therefore, the hydrostatic pressure of the effective liquid column would have to be calculated with the density at the corresponding mean temperature. To simplify the calculation, and to be on the safe side, the density is calculated for a temperature that is by a difference of ΔT_0 lower than the average liquid temperature, ϑ_k. A value of $\Delta T_0 = 10\,\text{K}$ was chosen for this study, valid for all states. The hydrostatic pressure at a location *X* in State *k* is:

$$\Delta p_{st,X,k} = \rho\left(\vartheta_k - \Delta T_0\right) g \Delta h_x \tag{1}$$

The atmospheric pressure, p_{Atm}, is calculated using the standard atmosphere model (Thomas and Freytag 2009) as a function of altitude, h_0:

$$p_{Atm} = 101325\left(1 - \frac{6.51 \cdot 10^{-3} h_0}{288.15}\right)^{5.255} \tag{2}$$

It is assumed that the pressure gage, the safety valve, and the integration point are on the same level (see Figure 3). The pressure at the integration point is called system pressure. The system pressure at an arbitrary State *F* is defined as follows:

$$p_{I,k} = p_F - \Delta p_{st,I,k} \tag{3}$$

Overpressures at the location *X* in the state *k* are expressed as in Equation (4).

$$\hat{p}_{X,k} = p_{X,k} - p_{Atm} \tag{4}$$

The change in circuit temperature from State 1 to State *k* results in a corresponding change in the MEV gas volume ΔV_{1-k}, which is a function of the density ρ, average temperature ϑ, and expansion factor β of the piping material. The gas volume change within the MEV can be calculated using Equation (5), if detailed information on volume shares, $V_{C,i}$, and temperatures is available.

$$\Delta V_{1-k} = \sum_{i=1}^{n} V_{C,i}\left[\frac{\rho_{\vartheta_{i,1}} - \rho_{\vartheta_{i,k}}}{\rho_{\vartheta_{i,1}}} - 3\beta_i\left(\vartheta_{i,k} - \vartheta_{i,1}\right)\right] \tag{5}$$

In most cases, the circuit consists largely of a single type of material. Assuming a linear relationship between density and temperature, the average density in State *k* can be calculated as a function of the volume-averaged temperature, and the gas volume change within the MEV is calculated as follows:

$$\Delta V_{1-k} = V_C \frac{\rho_1 - \rho_k}{\rho_1} - 3\beta \cdot \Delta \vartheta_{1-k} \tag{6}$$

To be on the safe side when dimensioning the MEV volume, some of the methods discussed below calculate the densities based on the highest and lowest temperatures that can occur in a circuit, instead of average temperatures. The resulting gas volume change is always greater than according to Equation (6) and is denoted by $\hat{V}_{1-k}$.

The density and the vapor pressure of the heat-carrier liquid are calculated using the correlations presented in Appendix B.

1.4. State-of-the-art dimensioning of MEVs

The technical rules relevant to this study, including the work on which they were based, are described below.

Lockhart et al. (1953) derived a formula for sizing compression tanks based on the gas content transition between States 0, 1, and 2. In State 0, the gas state is characterized by the temperature, T_0, and the pressure, $p_0 = p_{\text{atm}} + p_e$, where p_e is the overpressure when the gas volume, V_0, comprises the tank volume, V_T, and a gas volume, V_r, released from the water by desorption owing to heating. This gas volume is set to a constant of two percent of the circuit volume, $V_r = 0.02 \cdot V_C$. After filling the circuit, the pressure is p_1, and the temperature is T_1. In this state, the circuit has the lowest average temperature, ϑ_1. In State 2, the average circuit temperature reaches the highest mean value, ϑ_2, and both the liquid volume of the hydronic system, V_S, and the piping material expand according to their expansion factors. The liquid expansion factor is defined by the relative density difference between States 1 and 2, $E_W = (\rho_1 - \rho_2)/\rho_1$. The piping expansion factor, $E_P = 3\beta(\vartheta_2 - \vartheta_1)$, is proportional to the temperature difference between States 1 and 2. The net expansion volume of the liquid, $\Delta V_{1-2} = V_C (E_W - E_P)$, is displaced into the tank, and the pressure and gas temperature rise to values, p_2 and T_2. Consequently, both the initial volume of the liquid inside the tank, V_{WT}, and the volume of the tank, V_T, increase proportional to their expansion factors, E_{WT} and E_T. The effect of vapor pressure is neglected, and the tank volume is calculated by applying the ideal-gas model to the transitions between the three states:

$$V_T = \frac{\Delta V_{1-2}}{\dfrac{p_0 T_1}{p_1 T_0} - \dfrac{p_0 T_2}{p_2 T_0} - \left(1 - \dfrac{p_0 T_1}{p_1 T_0}\right) E_{WT} + E_T} - V_r . \tag{7}$$

Several simplifications were made: The liquid volume within the tank is not significant compared with the volume of the circuit, and the tank-temperature change is typically much smaller than the circuit-temperature change. Therefore, the expansion factors E_T and E_{WT} were set to zero.

Based on the work of Lockhart et al. (1953), Coad (1980) presented simplified Equations (8) and (9), which were incorporated into ASHRAE (2020). Equation (8) is applicable to closed tanks with a gas/water interface, where the gas is at atmospheric pressure before filling:

$$V_T = \frac{\Delta \hat{V}_{1-2}}{\frac{p_{Atm}}{p_1} - \frac{p_{Atm}}{p_2}} \tag{8}$$

Equation (9) is applicable to precharged MEVs:

$$V_T = \frac{\Delta \hat{V}_{1-2}}{1 - \frac{p_1}{p_2}} \tag{9}$$

To clarify the sizing method implemented in ASHRAE (2020), the works of Lockhart et al. (1953) and Coad (1980) were discussed by Taylor (2003, 2016). In accordance with these sources, the preset pressure should be equal to the filling pressure at the lowest circuit temperature. However, this statement requires further clarification. Pressure measurements are subject to uncertainties. If the pressure gages used to determine preset and reference pressures display the same values, the real preset pressure may be higher than the real reference pressure. Consequently, there would be no liquid within the MEV, and the membrane would not be able to transmit gas pressure to the circuit. The reference pressure would depend on the elasticity of the circuit-material and the compressibility of the circuit content. It can drop to a level where cavitation and entry of air can occur. To avoid this, the PMS must be installed with an automatic makeup system that provides a complementary pressure-boundary condition. In systems without an automatic makeup system, a minimum liquid volume must be present on the liquid side of the membrane. Consequently, the reference pressure must always exceed the preset pressure.

Pop et al. (2015) derived an improved model for the required MEV volume that distinguishes between preset pressure, p_0, and minimum reference pressure, p_1. Consequently, the dimensioning equation was based on the three pressure states of the gas volume in the MEV, as in the model derived by Lockhart et al. (1953). The model also considers a possible MEV temperature change from State 1 to State 2. Applying the ideal-gas model to the transition between the three states results in Equation (10), where a pre-factor of 1.1 is used to ensure safety.

$$V_T = 1.1 \frac{\Delta V_{1-2}}{\frac{p_0}{p_1} - \frac{p_0 T_2}{p_2 T_0}}. \tag{10}$$

The maximum pressure p_2 was defined as the opening pressure of the safety valve. The minimum pressure was defined by Equation (11), so that the pressure at the high point of the circuit exceeded the atmospheric pressure using the pressure allowance of $\Delta p_z = 20$ kPa .

$$p_1 = p_{Atm} + \Delta p_{st,H,1} + \Delta p_z \tag{11}$$

The atmospheric pressure was assumed to be the $p_{Atm} = 100$ kPa .The preset pressure p_0 is not explicitly defined; however, it is lower than the minimum reference pressure p_1.

VDI 4708-1 (2012) and SWKI (2020) regulations and the DIN EN 12828 (2014) standard also distinguish between the minimum system- and preset-pressures. However, the MEV temperature was considered constant. Moreover, the equations were formulated for overpressure, and the atmospheric pressure was set to $p_{Atm} = 100$ kPa . Expansion of the piping material is neglected, and the liquid density in State 2 is calculated at the maximum temperature.

In the author's opinion, VDI 4708-1 (2012) is the most advanced of the established methods because it considers the occurrence of a liquid process volume, ΔV_Z , that is displaced into the MEV over a short period of time, in addition to the volume change due to thermal expansion. Process volumes can occur for two reasons: 1) During vacuum degassing cycles, part of the degassing tank volume is transferred into the circuit, and a corresponding volume is displaced into the MEV. 2) When the solar thermal circuits stagnate , the collectors generate steam to fill the entire collector field and parts of the adjoining pipes. The liquid volume corresponding to the steam volume is displaced into the MEV. Details regarding the stagnation of solar thermal circuits are provided by Hausner et al. (2003); Scheuren (2008) and Eismann et al. (2021).

The dimensioning method (VDI 4708-1 2012) is briefly discussed below. To facilitate comparison with the new dimensioning method defined in Section 2, equations are formulated with absolute pressures. The hydrostatic pressures at the location x are calculated based on the density at the minimum occurring temperature in State 1:

$$\Delta p_{st,x,k} = \rho\left(\vartheta_{1,\min}\right) g \Delta h_x \tag{12}$$

A liquid reserve volume, V_V, within the MEV is required to transfer gas pressure to the circuit and compensate for minor liquid losses that might occur within a maintenance interval. The reserve volume must be at least a fraction, $\gamma_C = 0.005$, of the circuit volume and not smaller than the minimum volume, $V_{\mathrm{Res,min}}$, of 3 L:

$$V_V = \max\left\{V_{\mathrm{Res,min}}\,;\,\gamma_C \cdot V_C\right\} \tag{13}$$

The operational pressure range of the MEV is defined by the initial pressure p_1 and the final pressure p_2 . The initial pressure is defined such that the pressure at the highpoint of the circuit exceeds the atmospheric pressure and the vapor pressure by two pressure allowances. The first pressure allowance, $\Delta p_{z1} \geq 20$ kPa , is to compensate for gas losses that might occur during

maintenance intervals. The second pressure allowance, $\Delta p_{z2} \geq 30\,\text{kPa}$, is used to create a liquid reserve volume within the MEV. If the integration point is at the suction-side of the pump, the initial pressure is calculated as follows:

$$p_1 \geq p_{1,\min} = \max\left\{p_{Atm}, p_v\right\} + \Delta\hat{p}_{st,H,1} + \Delta p_{z,1} + \Delta p_{z,2}\,. \tag{14}$$

The preset pressure, p_0, is smaller than the initial pressure by Δp_{z2}:

$$p_0 \geq \max\left\{p_{Atm}, p_v\right\} + \Delta\hat{p}_{st,H,1} + \Delta p_{z1}\,. \tag{15}$$

If the integration point is at the suction-side, the pump pressure, Δp_P, must be added to both Equations (14) and (15). Pipe friction is neglected.

The final pressure within the MEV, p_2, must not exceed the maximum pressure, $p_{\max}$, which is defined by the opening pressure of the safety valve, p_{SV}, minus the reseating pressure difference, Δp_{SV}, and the hydrostatic pressure difference between MEV and safety valve:

$$p_2 \leq p_{2,\max} = p_{SV} - \Delta p_{SV} + \Delta\hat{p}_{st,I,1}\,. \tag{16}$$

The dimensioning method is based on the relations between the three States 0, 1, and 2 of the gas volume within the MEV. State 0 describes an empty, precharged MEV. In State 1, the MEV contains the reserve volume, V_V, and the circuit temperature is at a minimum. In State 2, the gas within the MEV is isothermally compressed by the volume change, $\Delta V_{1-2}^{\max}$, and the process volume ΔV_Z, if applicable. The minimum nominal volume of the MEV is:

$$V_{N,\min} = \left(V_V + \Delta\hat{V}_{1-2} + \Delta V_Z\right)\frac{p_{\max}}{p_{\max} - p_0}\,. \tag{17}$$

From the standard sizes offered by the supplier, the MEV with $V_N > V_{N,\min}$ must be selected, so that the actual reserve volume, $V_V' = V_N \cdot \Delta p_{z2} / p_1$, is equal or larger than required, and the pressure requirement, Equation (16) is fulfilled. Tables and diagrams based on Equation (18) can be used for an approximate estimate of the filling state of a circuit.

$$p_F = \frac{p_0 V_N}{V_N - V_V' - \Delta V_{1-F}}\,. \tag{18}$$

1.5. Definition of research questions and goals

Established dimensioning methods contain two major limitations:

1. The measurement uncertainties of the preset and system pressures are not considered.
2. The influence of the MEV temperature on the preset gas and system pressures is not considered.

Therefore, it is not possible to assess the filling state of a circuit with sufficient accuracy, based on readings of the system pressure and circuit temperatures. This may result in incorrect pressures being set for commissioning or maintenance. In addition, maintenance may not be conducted at all, owing to a lack of objective information. Consequently, hydronic system malfunctions can be traced back

to poorly designed (Polchinski 2013) or faulty PMS (Certuse 2012; de Keizer et al. 2008). Malfunctions are noticeable by a lack of system pressure (Chen et al. 2018), which leads to air entrainment, resulting in flow blockages (Gallagher 2022; Ho 2021) and corrosion (Davis 1987). These analyses clearly show the need for an improved dimensioning method that is also suitable for assessing the filling state during maintenance.

Solar thermal circuits require a more advanced dimensioning method because the process volume is generally higher than the thermal volume change of the liquid. The MEV temperature can change considerably because the volume of the intermediate vessel is usually much smaller than the volume of the displaced hot liquid. The aim of this study is to generalize a method developed for solar thermal systems (Eismann 2017) in the following way:

1. The dimensioning method applies to any hydronic systems, such as heating networks, cooling circuits, and solar thermal circuits.
2. The effect of MEV temperature on the preset and system pressures is accounted for.
3. The following measurement uncertainties can be accounted for:
    a. Preset pressure and system pressure
    b. MEV temperature and average circuit temperature
4. A practical open-source software tool based on the generalized method is provided.

2. Derivation of an extended dimensioning method

2.1. Reserve volumes, pressure allowances, and uncertainties of pressure measurements

The reserve volume consists of two parts. A minimum reserve volume, $V_{\mathrm{Res},0}$, ensures that the gas pressure within the MEV can be transmitted into the circuit. It is defined as a fraction, γ_N, of the MEV volume, which may depend on the membrane type and vessel size:

$$V_{\mathrm{Res},0} = \gamma_N \cdot V_N \tag{19}$$

Because no information is currently available, a value of $\gamma_N = 0.01$ is suggested. To compensate for the minor liquid losses, an additional, usable reserve volume, V_{Res}, is defined similarly to Equation (13):

$$V_{\mathrm{Res}} = \max\left\{V_{\mathrm{Res,min}}\,;\,\gamma_C \cdot V_C\right\}. \tag{20}$$

The minimum reserve volume, $V_{\mathrm{Res,min}}$, and the fraction of the circuit volume, γ_C, must be selected according to the system requirements. The pressure allowance for the compensation of preset pressure losses, Δp_{z1}, is defined as in VDI 4708. If the pressure allowance Δp_{z1} approaches zero and the reserve volume V_{Res} diminishes, the minimum pressure at any point in the circuit should still exceed the atmospheric pressure or vapor pressure by a finite amount. This amount is specified by a new pressure allowance, Δp_{z0}, which was set to 30 kPa in this study.

The pressure gages used to measure the preset pressure typically have an uncertainty, δp_{P0}, of 0.05 bar. An uncertainty of the gas temperature within an MEV of $\delta T = 2.5\,\mathrm{K}$ is assumed. The total uncertainty of the preset pressure is calculated as follows:

$$\delta p_0 = \delta p_{p_0} + \frac{\partial p}{\partial T}\delta T = \delta p_{p_0} + \frac{p}{T}\delta T\,. \tag{21}$$

Figure 4 shows the total uncertainty for a typical preset-pressure range based on these values. For the dimensioning of MEVs, a practical value of $\delta p_0 = 10\,\mathrm{kPa}$ is recommended.

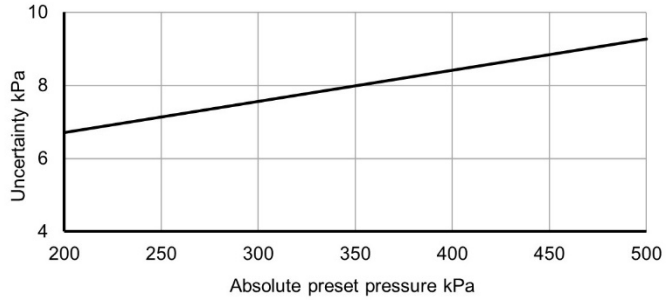

Figure 4. Uncertainty in preset-pressure measurements.

The system-pressure uncertainty depends on the accuracy class and the measuring range of the pressure gage.

2.2. Extremal states, and dimensioning procedure

The dimensioning procedure is based on the requirements and boundary conditions formulated for three extremal states of the circuit and four extremal states of the MEV. These states are qualitatively characterized in Table 1.

Table 1. Extremal states of the circuit and MEV

State	Circuit	MEV
0	-	Preset pressure, p_0, at the lowest possible temperature of the gas volume, T_0.
1	Lowest average circuit temperature, ϑ_1. No process volume.	Gas pressure, p_1, at the lowest possible temperature of the gas volume in State 1, $T_1 = T_0$.
2	Highest average circuit temperature, ϑ_2, during normal operation. No process volume.	Gas pressure, p_2, at the lowest possible temperature of the gas volume in State 2, $T_2 \geq T_0$.
3	Highest average circuit temperature, ϑ_3. Process volume ΔV_Z occurs.	Gas pressure, p_3, at the highest possible temperature of the gas volume in State 3, $T_3 \geq T_0$.
F	Average circuit temperature, ϑ_F, at an arbitrary state between extremal States 1 and 2.	Gas pressure, p_F, at an arbitrary temperature of the gas volume, $T_F \geq T_0$.

Figure 5 qualitatively illustrates the dependence of the system pressure on the average circuit temperature (black line) and the temperature of the gas volume (red line). The MEV temperature change between States 1 and 2 can be significant, when caused by seasonal temperature changes or boiler waste heat, for example. In addition, the temperature can change because of the displacement of liquid from the circuit into the MEV.

The process volume caused by the voids created during the vacuum-degassing cycles can be superimposed on all states between extremal States 1 and 2, as indicated by the black dashed lines. However, only the transition from State 2 to 3 is relevant to the dimensioning.

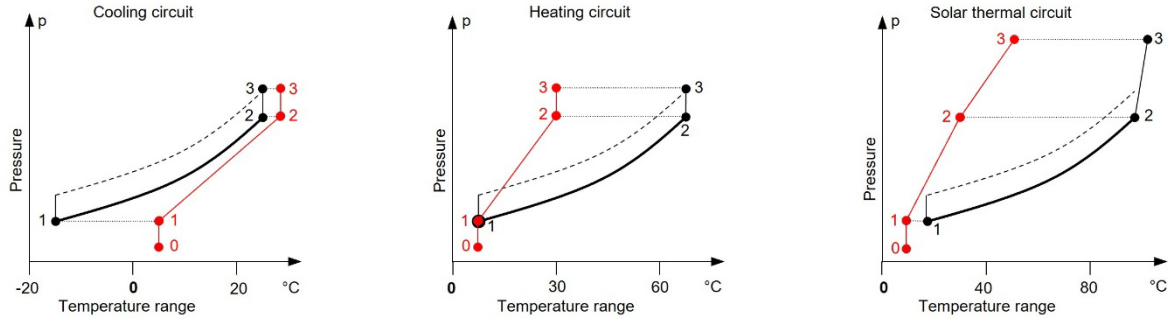

Figure 5. Pressure within the MEV as a function of the average circuit temperature (black lines) and MEV temperature (red lines) for cooling, heating, and solar thermal circuits.

Figure 6 illustrates the dimensioning procedure.

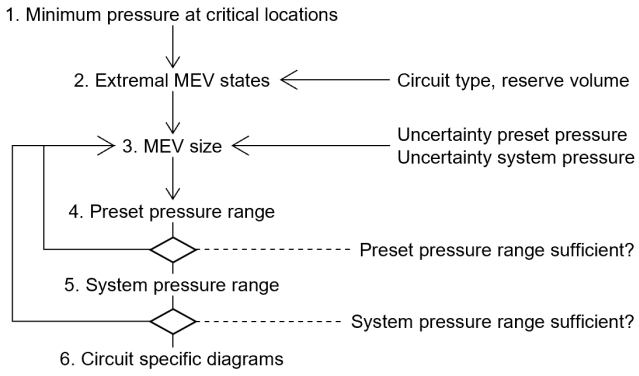

Figure 6. Dimensioning procedure for MEVs.

2.3. Minimum-required and maximum-permitted pressures within the circuit

For the minimum pressure in State 1, air ingress, liquid evaporation during normal operation, and cavitation must be avoided. For safe and reliable operation, the minimum pressure at any point in the circuit must exceed the atmospheric pressure, p_{atm}, and the vapor pressure, p_v, by a finite amount, as defined by the pressure allowance Δp_{z0}. It is sufficient to formulate this requirement for the critical locations of the circuit. For cooling and heating circuits, these are the highpoint of the

circuit and the pump inlet. Both are characterized by height differences, h_H , and h_P , as shown in Figure 2. With solar thermal circuits, the collector field can represent a local high point, h_S , and the temperatures at the highpoints, h_S and h_H , can be different. With these considerations, the minimum pressure at the highpoint of any hydronic systems in State 1 can be defined according to Equations (22). Equation (23) additionally applies to solar thermal systems.

$$p_{H,1} \geq p_{H,1,\min} = \max\left\{p_{v,H,1}\,;\,p_{Atm}\right\} + \Delta p_{z0} \tag{22}$$

$$p_{S,1} \geq p_{S,1,\min} = \max\left\{p_{v,S,1}\,;\,p_{Atm}\right\} + \Delta p_{z0} \tag{23}$$

The pressure at the pump inlet must not be less than the minimum pressure according to the data sheet, which is a function of the liquid temperature at the pump inlet in State 1:

$$p_{P,1} \geq p_{P,\min}\left(\vartheta_{P,1}\right). \tag{24}$$

With solar thermal circuits, the flow distribution within a large, branched collector field is not perfectly homogeneous. This will lead to a corresponding temperature distribution at the collector's outlets. The vapor pressure, $p_{v,S,2}$, is calculated for the highest collector exit temperature, which exceeds the mixing temperature at the outlet of the collector field by a temperature difference ΔT_S. If the temperature deviation cannot be obtained by a pipe-network analysis, calculation with a practical value of $\Delta T_S = 5\,\mathrm{K}$ is suggested. Equations (25) and (26) define the minimum pressure at the highpoints in State 2:

$$p_{H,2} \geq p_{H,2,\min} = \max\left\{p_{v,H,2}\,;\,p_{Atm}\right\} + \Delta p_{z0} \tag{25}$$

$$p_{S,2} \geq p_{S,2,\min} = \max\left\{p_{v,S,2}\,;\,p_{Atm}\right\} + \Delta p_{z0} \tag{26}$$

The pump inlet pressure in State 2 is defined analogously to Equation (24):

$$p_{P,2} \geq p_{P,\min}\left(\vartheta_{P,2}\right) \tag{27}$$

The maximum pressure at the location of the safety valve is defined as in (VDI 4708-1 2012):

$$p_{SV,\max} = p_{SV} - \Delta p_{SV} \tag{28}$$

2.4. Extremal pressures within the MEV

The pressure in the MEV differs from the pressure at the high point by the hydrostatic pressure of the liquid column, the friction pressure loss, and, depending on the location of the integration point, the pump pressure. If the integration point is on the pressure side of the pump, the pressure within the MEV must be increased by the friction-pressure losses that occur in the circuit sections, *i*, between the integration point and the highpoint:

$$\Delta p_{f,H} = \sum_{i=1}^{i_H}\left|\Delta p_{f,i}\right| \quad ; \quad \Delta p_{f,S} = \sum_{i=1}^{i_S}\left|\Delta p_{f,i}\right|. \tag{29}$$

If the integration point of the MEV is on the suction side of the pump, the pump pressure Δp_P must be subtracted:

$$\Delta p_H = \sum_{i=1}^{i_H} \left| \Delta p_{f,i} \right| - \Delta p_P \quad ; \quad \Delta p_S = \sum_{i=1}^{i_S} \left| \Delta p_{f,i} \right| - \Delta p_P \,. \tag{30}$$

Whether the pump is running in States 1, 2, or 3 depends on the circuit type. The state of the pump in the State, $k \in \{1..3\}$, of the circuit is indicated by the variable, $\delta_{P,k} \in \{0,1\}$. The location of the integration point is defined by the parameter, $\delta_I \in \{0,1\}$. Table 3 lists the recommended values.

Table 2 Recommended values for the pump state variable and the integration point parameter.

	Pump state variable, δ_P			Integration point, δ_I	
State	1	2	3	Suction	Pressure
Cooling	1	1	1	1	0
Heating	1	1	1	1	0
Solar	1	1	0	0	1

Using these definitions, Equations (29) and (30) can be combined, resulting in the following Equations:

$$\Delta p_{H,k} = \delta_{P,k} \left(\Delta p_{f,H} - \delta_I \Delta p_P \right) \quad ; \quad \Delta p_{S,k} = \delta_{P,k} \left(\Delta p_{f,S} - \delta_I \Delta p_P \right). \tag{31}$$

In State 1, the minimum pressure inside the MEV is defined by the minimum pressures at the high points of the circuit and the hydrostatic pressure of the respective liquid columns. Equation (31) yields a negative value if the integration point is on the suction side. Therefore, in the state where the pump is typically switched on, the case in which the pump is switched off must also be considered. For convenience, Equation (32) is used for all types of circuits, while only the relevant terms contribute. When the pump is running, the third line of this equation accounts for the inlet pressure condition.

$$p_1 = \max \begin{Bmatrix} p_{H,1,\min} + p_{g,H} + \Delta p_{H,1} \,;\, p_{H,1,\min} + p_{g,H} \\ p_{S,1,\min} + p_{g,S} + \Delta p_{S,1} \,;\, p_{S,1,\min} + p_{g,S} \\ \delta_{P,1} \left(p_{P,1} + p_{g,P} \right) \end{Bmatrix} \tag{32}$$

The minimum pressure in State 2 is defined by Equation (33), which has the same structure as Equation (32), but is evaluated at different temperatures:

$$p_2 = \max \begin{Bmatrix} p_{H,2,\min} + p_{g,H} + \Delta p_{H,2} \,;\, p_{H,2,\min} + p_{g,H} \\ p_{S,2,\min} + p_{g,S} + \Delta p_{S,2} \,;\, p_{S,2,\min} + p_{g,S} \\ \delta_{P,2} \left(p_{P,2} + p_{g,P} \right) \end{Bmatrix} \tag{33}$$

The maximum pressure in the MEV occurs in State 3. It is defined by the maximum pressure of the safety valve, Equation (28), and the hydrostatic pressure of the liquid column between the MEV and the safety valve. Based on these considerations, the maximum pressure is defined as follows:

$$p_{\max} = \left(p_{SV,\max} + p_{g,SV} \right) \tag{34}$$

2.5. Determining the MEV volume

In State 1, the average liquid temperature is at the minimum, and the MEV contains the smallest amount of liquid. If the entire usable reserve volume is exhausted, for example due to leaks or other losses, the MEV must still contain the minimum reserve volume $V_{\mathrm{Res},0}$. Therefore, the minimum gas volume $V_{1,\min}$ in State 1 and the minimum volume $V_{N,\min}$ of the empty MEV are related as follows:

$$V_{N,\min} = V_{1,\min} + V_{\mathrm{Res},0}\,. \tag{35}$$

First, the minimum gas volume, $V_{1,\min}$, is determined. The unknown preset pressure at the reference temperature, T_0, is p_0. The change from the precharged state of the empty MEV to State 1 is considered isothermal and must satisfy the following condition:

$$p_0 V_{N,\min} \geq p_1 V_{1,\min}\,. \tag{36}$$

During the transition from State 1 to State 2, the gas volume is further compressed by ΔV_{1-2}. Temperature changes can also be a part of the change of state. Consequently, States 1 and 2 are related as follows:

$$\frac{p_0 V_{N,\min}}{T_1} \geq \frac{p_2 \left(V_{1,\min} - \Delta V_{1-2} \right)}{T_2} \tag{37}$$

Because it is not yet known which State, 1 or 2, is relevant, in both Equations (36) and (37), the weaker relationships $\geq$ must be used instead of equality. In State 3, the gas volume is compressed by ΔV_{1-3}, and the gas volume temperature may have increased to T_3. In this state, the usable reserve volume, V_{Res}, is also assumed to be present. Furthermore, the process volume, ΔV_Z, is considered in State 3. Accordingly, State 0 of the empty, precharged MEV and State 3 are related by the following equation:

$$\frac{p_0 V_{N,\min}}{T_0} = \frac{p_{\max} \left(V_{1,\min} - \Delta V_{1-3} - V_{Res} - \Delta V_Z \right)}{T_3} \tag{38}$$

Here, equality must be applied because the maximum pressure $p_{\max}$ defines the upper limit. By defining $p_3 = p_{\max} T_1 / T_3$, Equation (38) can be rewritten as

$$p_0 V_{N,\min} = p_3 \left(V_{1,\min} - \Delta V_{1-3} - V_{Res} - \Delta V_Z \right). \tag{39}$$

Subsequently, Equations (36), (37), and (39) are solved for the minimum gas volume in State 1:

$$V_{1,\min} = \max \left\{ \frac{p_3 \left(\Delta V_{1-3} + V_{\mathrm{Res}} + \Delta V_Z \right)}{p_3 - p_1} ; \frac{p_3 T_2 \left(\Delta V_{1-3} + V_{\mathrm{Res}} + \Delta V_Z \right) - p_2 T_1 \Delta V_{1-2}}{p_3 T_2 - p_2 T_1} \right\}. \tag{40}$$

With $V_{1,\min}$ from Equation (40), Equations (35) can be solved for the minimum MEV volume, and Equation (39) can be solved for the preset pressure:

$$p_0 = \frac{p_3\left(V_{1,\min} - \Delta V_{1-3} - V_{Res} - \Delta V_Z\right)}{V_{N,\min}}. \tag{41}$$

From the standard sizes offered by the supplier, the MEV with the next larger volume, $V_N > V_{N,\min}$, is selected. Whether this volume is sufficient depends on the pressure-measurement uncertainties and the desired, usable, system-pressure range.

2.6. Theoretical range for the preset pressure

Because $V_N > V_{N,\min}$, a specific preset pressure range is valid, instead of the one value calculated by Equation (41). The upper limit is defined by the requirement that the MEV in state 1 must contain at least the minimum reserve volume, $V_{\mathrm{Res},0}$, so that the gas volume is at its maximum:

$$V_{1,\max} = V_N - V_{\mathrm{Res},0}. \tag{42}$$

Replacing $V_{1,\min}$ with $V_{1,\max}$, and $V_{N,\min}$ with V_N in Equation (41) results in the theoretical upper limit for the preset pressure:

$$p_{0,\max,\mathrm{theor}} = \frac{p_3\left(V_{1,\max} - \Delta V_{1-3} - V_{Res} - \Delta V_Z\right)}{V_N}. \tag{43}$$

Replacing $V_{1,\max}$ in Equation (43) by $V_{1,\min}$ from Equation (40) yields the theoretical lower limit for the preset pressure:

$$p_{0,\min,\mathrm{theor}} = \frac{p_3\left(V_{1,\min} - \Delta V_{1-3} - V_{Res} - \Delta V_Z\right)}{V_N}. \tag{44}$$

For the theoretical upper limit of the preset pressure, only one particular pressure, p_F, satisfies all three conditions defined in Equations (36), (37), and (39). The same is true for the theoretical lower limit of the preset pressure. There is an optimum preset pressure where the admissible range of pressures, p_F, is widest. This optimum preset pressure is defined by either Equation (36) or (37), with $V_{1,\max}$ instead of $V_{1,\min}$ and V_N instead of $V_{N,\min}$, as follows:

$$p_{0,\mathrm{opt}} = \max\left\{\frac{p_1 V_{1,\max}}{V_N}; \frac{p_2 T_1\left(V_{1,\max} - \Delta V_{1-2}\right)}{V_N T_2}\right\} \tag{45}$$

2.7. Theoretical range for the filling pressure

The state of a precharged MEV and an arbitrary filling is related by Equation (46), where the gas volume V_1 in state 1 is yet unknown.

$$p_0 V_N = p_F\left(V_1 - \Delta V_{1-F} - V_{\mathrm{Res}}\right)\frac{T_1}{T_F}. \tag{46}$$

The state of the precharged MEV and the three extremal states are related through Equations (36), (37), and (39), but with V_N instead of $V_{N,\min}$, and a preset pressure in the range of $p_{0,\min,\lim} \le p_0 \le p_{0,\max,\lim}$:

$$p_0 V_N \ge p_1 V_1 \tag{47}$$

$$p_0 V_N \ge p_2 \frac{T_1}{T_F}\left(V_1 - \Delta V_{1-2}\right) \tag{48}$$

$$p_0 V_N = p_3 \left(V_1 - \Delta V_{1-3} - V_{\mathrm{Res}} - \Delta V_Z\right) \tag{49}$$

First, Equation (49) is solved for the gas volume in State 1:

$$V_1 = \frac{p_0 V_N}{p_3} + \Delta V_{1-3} + V_{\mathrm{Res}} + \Delta V_Z \,. \tag{50}$$

Inserting V_1 from Equation (50) into Equation (46) and rearranging results in the theoretical upper limit of the filling pressure as a function of the preset pressure:

$$p_{F,\max,\mathrm{theor}} = \frac{p_3 p_0 V_N T_F}{\left[p_0 V_N + p_3\left(\Delta V_{1-3} + \Delta V_Z - \Delta V_{1-F}\right)\right] T_1} \tag{51}$$

To calculate the lower limit of the filling pressure, two regions of preset pressure must be considered. For a preset pressure above the optimum value, the conditions for States 1 and 2 are continually satisfied, and the gas volume is defined by Equation (42). Inserting $V_{1,\max}$ from Equation (42) into Equation (46) and rearranging results in the lower limit of the MEV pressure:

$$p_{F\,\min,\mathrm{theor}} = \frac{p_0 V_N T_F}{\left(V_N - V_{\mathrm{Res},0} - V_{\mathrm{Res}} - \Delta V_{1-F}\right) T_1} \quad ; \quad p_0 > p_{0,opt} \tag{52}$$

For a preset pressure equal or below the optimum value, the gas volume must be determined using Eqs. (47) and (48).

$$V_1 = \min\left\{\frac{p_0 V_N}{p_1}; \frac{p_0 V_N}{p_2 T_1 / T_F} + \Delta V_{1-2}\right\}. \tag{53}$$

Inserting V_1 into Equation (46) yields the theoretical lower limit of the filling pressure:

$$p_{F\,\min,\mathrm{theor}} = \frac{p_0 V_N T_F}{\left(V_1 - \Delta V_{1-F} - V_{\mathrm{Res}}\right) T_1} \quad ; \quad p_0 \le p_{0,opt} \tag{54}$$

2.8. Practical range of preset and MEV pressures

The practical range of the preset pressure is defined by considering the uncertainty of the preset pressure and the pressure allowance, Δp_{z1}:

$$\begin{aligned} p_{0,\max} &= p_{0,\mathrm{opt}} - \delta p_0 \\ p_{0,\min} &= p_{0,\mathrm{opt}} - \delta p_0 - \Delta p_{z1} \end{aligned} \,. \tag{55}$$

The maximum preset pressure should be set at commissioning. The minimum limit of the preset pressure is lower than the practical minimum by the uncertainty:

$$p_{0,\min,\lim} = p_{0,\min} - \delta p_0 \tag{56}$$

The maximum filling pressure is defined by Equation (51), evaluated at the lowest permitted preset pressure, and reduced by the uncertainty δp_{sys} of the system pressure:

$$p_{F,\max} = p_{F,\max,\text{theor}}\Big|_{p_{0,\min}-\delta p_0} - \delta p_{\text{Sys}}\,. \tag{57}$$

The minimum filling pressure is defined by Equation (53) and (54), and is increased by the system pressure uncertainty:

$$p_{F,\min} = \max\left\{\begin{matrix} p_{F,\min,\text{theor}}\Big|_{p_{0,\min}-\delta p_0} \\ p_{F,\min,\text{theor}}\Big|_{p_{0,\text{opt}}} \end{matrix}\right\} + \delta p_{\text{sys}}\,. \tag{58}$$

If the difference between the maximum and minimum filling pressures is smaller than a predefined minimum difference, Δp_{sys}, the next larger MEV must be chosen, and the dimensioning must be repeated from Equation (42). The minimum filling pressure, where the usable reserve volume is zero, $p_{F,\min,empty}$ is also calculated using Equation (53) and (54), but with $V_{\text{Res}} = 0$.

The uncertainty of the average circuit temperature, δ_ϑ, is accounted by evaluating the equations at a correspondingly shifted temperature:

$$\begin{aligned} p_{F,\max'}\left(\vartheta_F\right) &= p_{F,\max}\left(\vartheta_F - \delta_\vartheta\right) \\ p_{F,\min'}\left(\vartheta_F\right) &= p_{F,\min}\left(\vartheta_F + \delta_\vartheta\right) \\ p_{F,\min,empty'}\left(\vartheta_F\right) &= p_{F,\min,empty}\left(\vartheta_F + \delta_\vartheta\right) \end{aligned} \tag{59}$$

3. Discussion and Validation

To rationally apply the proposed method and discuss its properties using examples, a software tool was programmed in Visual Basic for Applications (VBA) using Microsoft Excel. To illustrate the features of the dimensioning methods and the influence of certain parameters, three examples and their variants are defined in Table 4.

Table 3 Specifications of cooling, heating, and solar thermal circuits. Variants are indicated by indices A, and B.

Quantity	Symbol	Unit	Cooling	Heating	Solar
Circuit volume	V_C	l	2500	2000	1200
Heat transfer liquid	-	-	W-G	Water	W-G
Height difference MEV - highpoint	$h_H = h_S$	m	6	2	10
Opening overpressure of safety valve	p_{SV}	kPa	600	600	600
Pressure hysteresis of safety valve	Δp_{SV}	kPa	60	60	60
Integration point	-	-	suction	suction	pressure
Minimum average circuit temperature, State 1	ϑ_1	°C	-20	10	0

Maximum average circuit temperature, State 2	ϑ_2	°C	30	60	80
Maximum average circuit temperature, State 3	ϑ_3	°C	30	60	90
Maximum circuit temperature	$\vartheta_{C,2}$	°C	30	80	110
Maximum collector outlet temperature	$\vartheta_{S,2}$	°C	-	-	115
Pressure loss integration point – highpoint	$\Delta p_H ; \Delta p_S$	kPa	30	0	30
Pump pressure	Δp_P	kPa	60	60	60
Required pump inlet pressure, State 1	p_P	kPa	10	10	10
Required pump inlet pressure, State 2	p_P	kPa	10	40	40
Process volume	ΔV_Z	l	0	5	100
MEV temperature, State 1	$\vartheta_{MEV,1}$	°C	10	10	10
MEV temperature, State 2	$\vartheta_{MEV,2}$	°C	10	10	10
MEV temperature, State 3	$\vartheta_{MEV,3}$	°C	10_A, 30_B	30	30
Uncertainties of pressure measurement	$\delta p_{sys}, \delta p_0$	kPa	10	10_A, 15_B	10

To facilitate the discussion, the following settings are valid for all examples: The pump and the safety valve are at reference height. The pressure allowances were set as/to $\Delta p_{z0} = 20\,\text{kPa}$, $\Delta p_{z1} = 20\,\text{kPa}$, and $\Delta p_{z2} = 30\,\text{kPa}$. The minimum range between the minimum and maximum permitted system pressures was set to $\Delta p_{sys} = 40\,\text{kPa}$. An accuracy class of 1.6 was specified for the system-pressure gage, which resulted in an uncertainty of 10 kPa. The same uncertainty was assumed for the preset-pressure gage. The minimum reserve volume was defined as $V_{\text{Res},0} = 0.01 \cdot V_N$, whereas the usable reserve volume was defined using $V_{\text{Res,min}} = 0.005\,\text{m}^3$ and $\gamma_C = 0.01$. The nominal MEV volumes were selected from the standard series presented in Table 7 in Appendix B. Both the proposed method and the VDI method were used to determine the nominal MEV volume.

Water-glycol mixture (W-G) of the type TYFOCOR®LS (TYFOROP 2015) were used for the cooling and solar thermal circuits.

3.1. Cooling circuit

Variant A is distinguished by a constant MEV temperature of 10 °C. Figure 7 shows the preset- and system-pressure ranges where the circuit is in State 1, hence $T_F = T_1$. The curved triangle indicates the theoretical limit of the system pressure as a function of the preset pressure. The upper limit was calculated using Equation (51). The upper right corner (○), corresponds to Equation (43). The left corner (□) corresponds to Equation (44). The upper limit was calculated using Equation (51). The lower limit is defined by two curves for two regions of preset pressure: For a preset pressure equal or higher than the optimum preset pressure, the lower limit was calculated using Equation (52). For a preset pressure below the optimum preset pressure, the lower limit was calculated using Equation (54). The bend at the transition between the two curves occurs at the optimum preset

pressure, $p_{0,\mathrm{opt}}$, where the difference between upper and lower limit is largest. State 1, that is, the left-hand term in Equation (53), is relevant in this case. Therefore, Equation (54) yields an increase in the system pressure with a decrease in the preset pressure. The rectangle with dashed edges indicates the permissible range for the preset and system pressure, including pressure uncertainties. The rectangle with continuous lines defines the practical range of the preset and system pressure. The width of this rectangle corresponds to the pressure allowance, $\Delta p_{z1} = 0.2$ bar. The distances between the continuous and dashed edges equal the uncertainties of the preset and system pressure. The rectangle bounded by a dashed line defines the pressure ranges including the uncertainties of pressure measurements. The practical values of the maximum and minimum filling pressure are calculated using Equation (57) and (58), for the same preset pressure indicated by (●) and (■). At commissioning, the preset overpressure should be set to 1.08 bar, and the system overpressure should be set to 2.32 bar, as indicated by the callout in Figure 7.

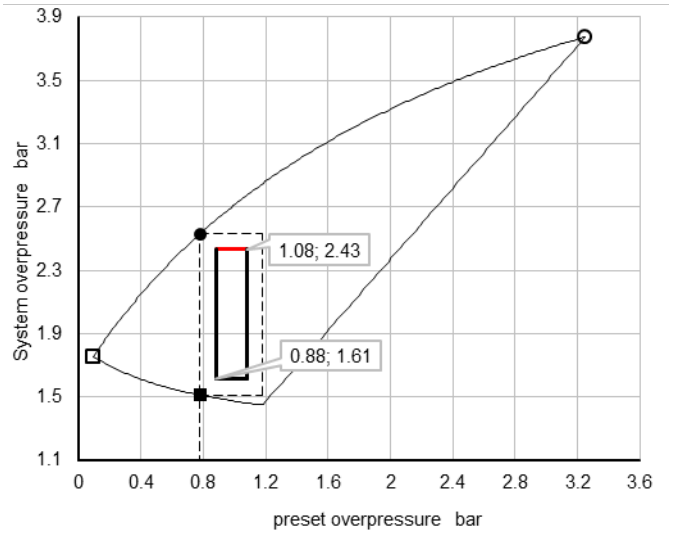

Figure 7. Preset pressure and system pressure ranges for State 1 of the cooling circuit, variant A.

Figure 8 shows the system overpressure range as a function of circuit temperature. The dashed red curve labeled (max) is calculated using Equation (57). The minimum value of 2.32 bar at 10 °C corresponds to the upper practical limit shown in Figure 7. The maximum pressure at an average circuit temperature of 30 °C is 5.3 bar. This value is smaller by the uncertainty of the system pressure than the maximum permitted value of 5.4 bar, as calculated using Equation (34). The dashed black curve labeled (min) is calculated using Equation (58). The minimum value of 1.61 bar corresponds to the lower practical limit shown in Figure 7. In the states indicated by this curve, the MEV contains the minimum reserve volume, $V_{\mathrm{Res},0}$, and the usable reserve volume, V_{Res}. The dotted black line labeled (empty) was also calculated using Equation (58), but based on evaluating Equation (54) for $V_{\mathrm{Res}} = 0$. Consequently, in the states indicated by this curve, the MEV contains only the minimum

reserve volume, $V_{\mathrm{Res},0}$. The uncertainty in determining the mean circuit temperature is accounted for by shifting the red curve to the right by the amount of the uncertainty and the black curves to the left by the same amount. The resulting curves, indicated by (max+), (min-), and (empty-) are to be used in practice.

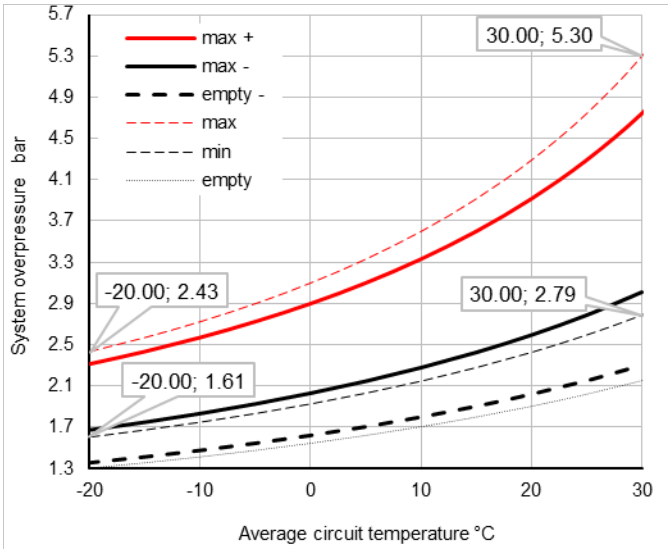

Figure 8 Cooling circuit, variant A. System pressure range as a function of average circuit temperature for a MEV temperature of 10 °C.

Table 4 allows to prove the validity of the proposed dimensioning method by comparing minimum required and maximum permitted values with calculated values, each with the worst-case uncertainties. Although the proposed method takes the uncertainties into account, it yields the same nominal MEV volume as the method according to VDI.

Table 4 Cooling circuit, variant A: MEV volume, and comparison of required/permitted and calculated values.

V_N	Proposed method	L	250	VDI	250
Quantity			State 1	State 2	State 3
$V_{\mathrm{res},0}$	Required	L	2.5	-	-
	Calculated at $p_{0,min,lim}$	L	48.0	-	-
	Calculated at $p_{0,opt}$	L	2.5	-	-
p_{H}	Required, $V_{res} = 0$	bar	0.20	0.20	-
	Calculated, pump off	bar	0.20	1.14	-
	Calculated, pump on	bar	0.50	1.44	-
p_{P}	Required	bar	0.50	0.90	-
	Calculated	bar	1.20	2.14	-
p_{max}	Permitted	bar	-	-	5.40
	Calculated	bar	-	-	5.40

The minimum reserve volume, $V_{\mathrm{Res},0}$, was calculated using Equation (54), with a usable reserve volume $V_{\mathrm{Res}} = 0$. As expected, the value based on the optimum preset pressure coincides with the required value. State 1 with the pump switched off is decisive for the pressure at the high point, which is indicated by highlighted cells. Because the integration point is on the suction side of the pump, the pressure at the high point increases when the pump is running. The calculated pressures at the pump inlet are above the required value in all states. The permitted and calculated pressure match.

In Variant B of the cooling circuit, a variable MEV temperature between 10 °C and 30 °C is considered. Both the proposed method and the VDI method yield an MEV volume of 250 L. At commissioning, the MEV can have any temperature within this range. Therefore, the preset overpressure must be calculated using Equation (59), and represented in Figure 9 for practical use:

$$p_0 = p_{0,\max}\, T_F / T_1 - p_{\mathrm{atm}}, \tag{60}$$

.

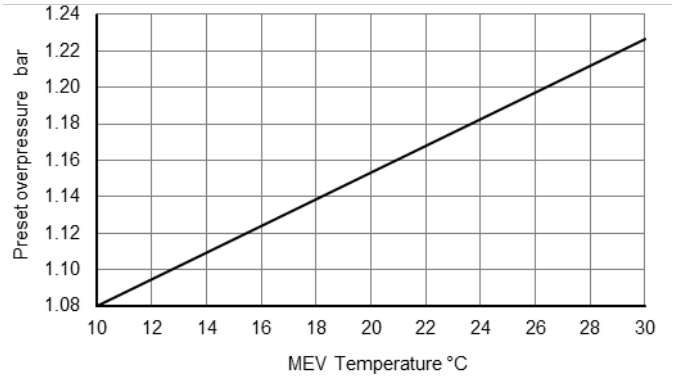

Figure 9. Cooling circuit, variant B: Preset overpressure as a function of MEV temperature.

Because the MEV Temperature can change, two linked diagrams are needed to assess the filling state, as shown in Figure 10. The left diagram shows the system pressure range as a function of the average circuit temperature when the MEV temperature is at $T_1 = 10$ °C. The transformation diagram on the right is used to determine the system pressure at different MEV temperatures. The application of the diagrams is illustrated by examples for commissioning and maintenance.

Commissioning: After filling and venting, the average circuit temperature is 20 °C, and the MEV has a temperature of 25 °C. In the first step, the maximum pressure of 3.6 bar can be read from the diagram, which is valid for a MEV temperature of 10 °C. In the second step, the pressure of 3.6 bar is mapped to the right diagram. Where the 3.6 bar line intersects with the 25 °C isotherm, the maximum pressure of 3.85 bar can be read from the horizontal axis.

Maintenance: The average circuit temperature is -10 °C, and the MEV temperature is 30 °C. The system overpressure is 2.3 bar. In the first step, the pressure of 2.3 bar is intersected with the 30 °C isotherm in the right diagram. In a second step, the intersection is mapped to the left diagram, where

a system overpressure of 2.2 bar is read from the vertical axis. The intersection of the 2.2 bar line and the circuit temperature of -10 °C indicates the filling state of the circuit. If the intersection lies on or between the curves indicated by (max +) and (min -), the filling state is okay. If the intersection lies on the dashed line indicated by (empty -), the usable reserve volume is used up, and maintenance is required.

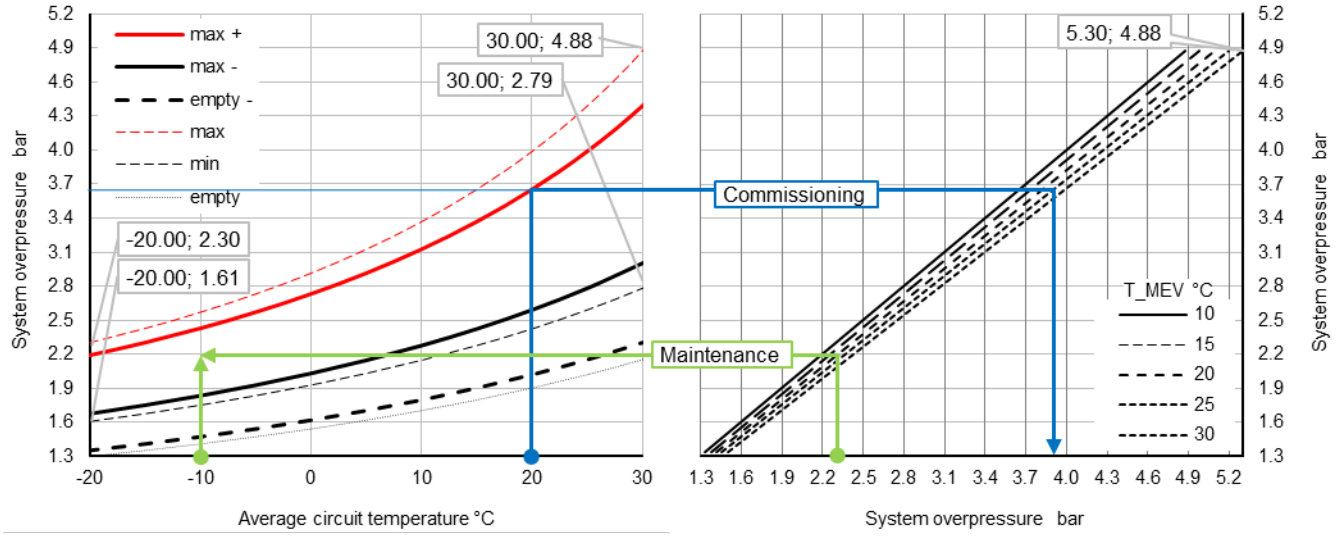

Figure 10 Cooling circuit, variant B: System pressure range for a MEV temperature of 10 °C. (left). System pressure for different MEV temperatures (right).

3.2. Heating circuit – variant a: pressure measurement uncertainty 10 kPa

Variant A of the heating circuit is distinguished by uncertainties of pressure measurements of 10 kPa. Thermal volume change of piping material is accounted for. Figure 11 shows the preset and system pressure ranges for State 1.

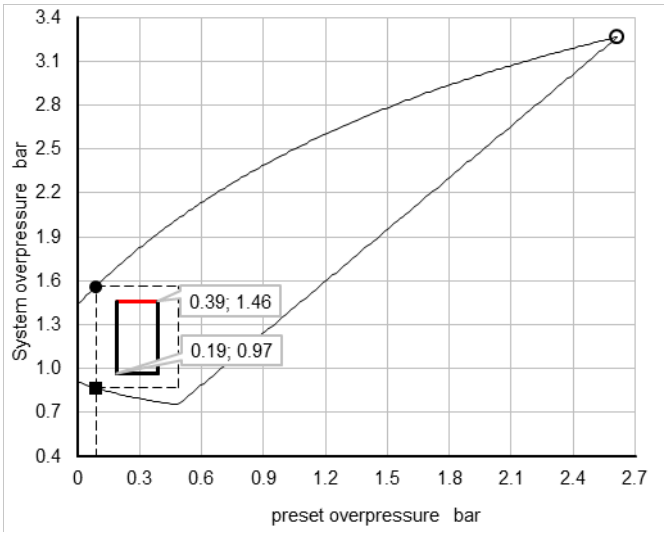

Figure 11. Heating circuit, Variant A: System pressure range as a function of average circuit temperature for a MEV temperature of 10 °C.

The diagram appears similar to that shown in Figure 7; however, it is shifted toward the lower pressures, because the highpoint is only 2 m above the reference level.

Figure 12 shows two linked diagrams similar to the cooling circuit, Figure 10. The maximum and minimum system overpressures of 1.46 and 0.97 bar correspond to the values shown in Figure 11. The maximum permitted overpressure at an average circuit temperature of 60 °C and a MEV temperature of 10 °C is 3.9 bar. At the maximum MEV temperature of 30 °C in State 3, the maximum system overpressure is 4.25 bar. The final overpressure of 5.3 bar (not shown in the diagram) is reached over a short period, when the process volume of 5 L occurs.

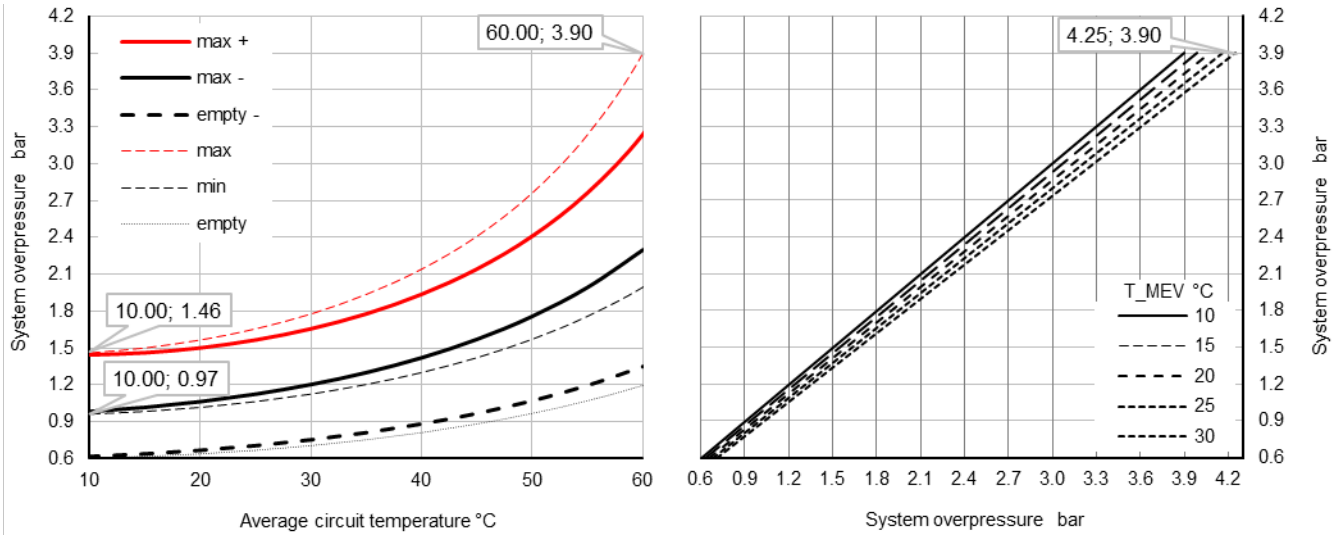

Figure 12. Heating circuit, variant A. Left diagram: System overpressure range as a function of average circuit temperature. Transformation diagram on the right: System overpressure for different MEV temperatures.

Table 5 shows minimum required and maximum permitted values, and the calculated values based on the worst-case uncertainties. The proposed method yields the same nominal MEV volume as the method according to VDI. The minimum inlet pressure in State 1 is decisive for the dimensioning, which is indicated by highlighted cells.

In Variant B, the thermal volume change of the circuit materials is neglected. Figure 13 shows the preset and system pressure ranges for State 1. The dashed line indicates the upper limit of the system overpressure for Variant A. Neither the preset pressure range nor the lower limit of the system overpressure are affected by neglecting the volume change of the circuit materials, because the expansion volume in these states is zero.

Table 5 Heating circuit, variant A: MEV volume, and comparison of required/permitted and calculated values.

V_N	Proposed method	L	140	VDI	140
Quantity			State 1	State 2	State 3
$V_{res,0}$	Required	L	1.4	-	-
	Calculated at $p_{0,min,lim}$	L	38.7	-	-
	Calculated at $p_{0,opt}$	L	1.4	-	-
p_H	Required, $V_{res} = 0$	bar	0.20	0.20	-
	Calculated, pump off	bar	0.30	1.01	-
	Calculated, pump on	bar	0.90	1.61	-
p_P	Required	bar	0.50	0.90	-
	Calculated	bar	0.50	1.21	-
p_{max}	Permitted	bar	-	-	5.40
	Calculated	bar	-	-	5.40

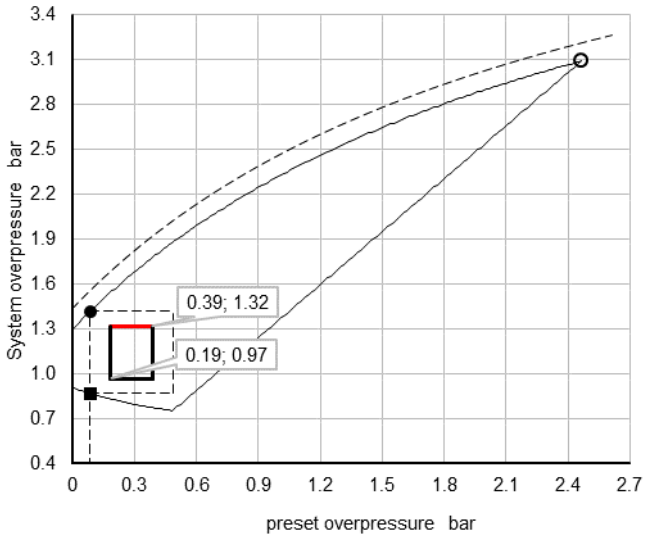

Figure 13 Heating circuit, Variant B: System pressure range as a function of average circuit temperature for a MEV temperature of 10 °C.

Figure 14 shows System overpressure range as a function of average circuit temperature for Variant B. For comparison, results for Variant A are shown and labeled (max A), (max + A). The admissible pressure range for Variant B is considerably smaller than for Variant A. The transformation diagram is not shown as it would be the same as the diagram on the right in Figure 12.

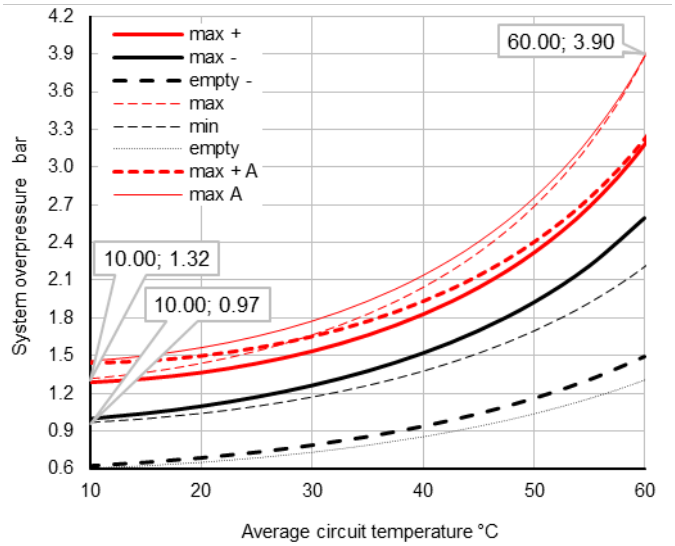

Figure 14 Heating circuit, Variant B. System pressure range as a function of average circuit temperature for a MEV temperature of 10 °C.

In Variant C, the thermal volume change of the circuit materials is considered, but the uncertainties of the pressure measurement are increased from 10 kPa to 15 kPa. Dimensioning using the proposed method results in the next largest MEV volume of 200 L.

3.3. Solar thermal circuit

In contrast to heating and cooling circuits, the integration point for solar thermal circuits is on the pressure side of the pump. Furthermore, the volume of liquid displaced into the MEV during stagnation is much larger than the volume owing to vacuum degassing. In Variant A, the increase of the MEV temperature from 10 °C to 30 °C in state 3 is considered. Figure 15 shows the preset-pressure and system-pressure ranges for State 1. The marker (x) at 0.67 bar indicates the preset overpressure, where the two terms in Equation (53) are equal, which results in Equation (60).

$$p_0 = \frac{\Delta V_{1-2}}{V_N \left(\frac{1}{p_1} - \frac{1}{p_2} \right)} \tag{61}$$

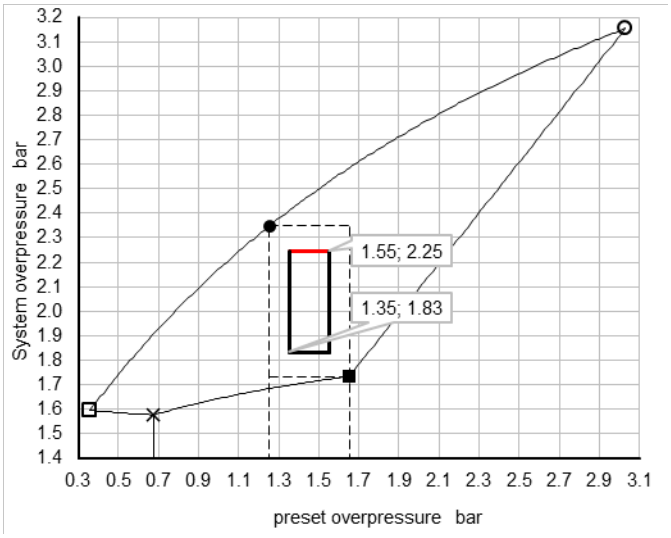

Figure 15. Variant A of the solar-thermal circuit: Preset and system pressure ranges for State 1

Figure 16 shows the linked diagrams of the specified, solar thermal circuit. An interesting feature is the significantly smaller increase in the system overpressure (approximately 0.7 bar, compared to the increase of approximately 2.4 bar with the heating circuit), because the process volume does not occur during State 1. A significantly larger pressure increase happens during stagnation, when the process volume of 100 L enters the MEV, and the temperature increases to 30 °C in State 3.

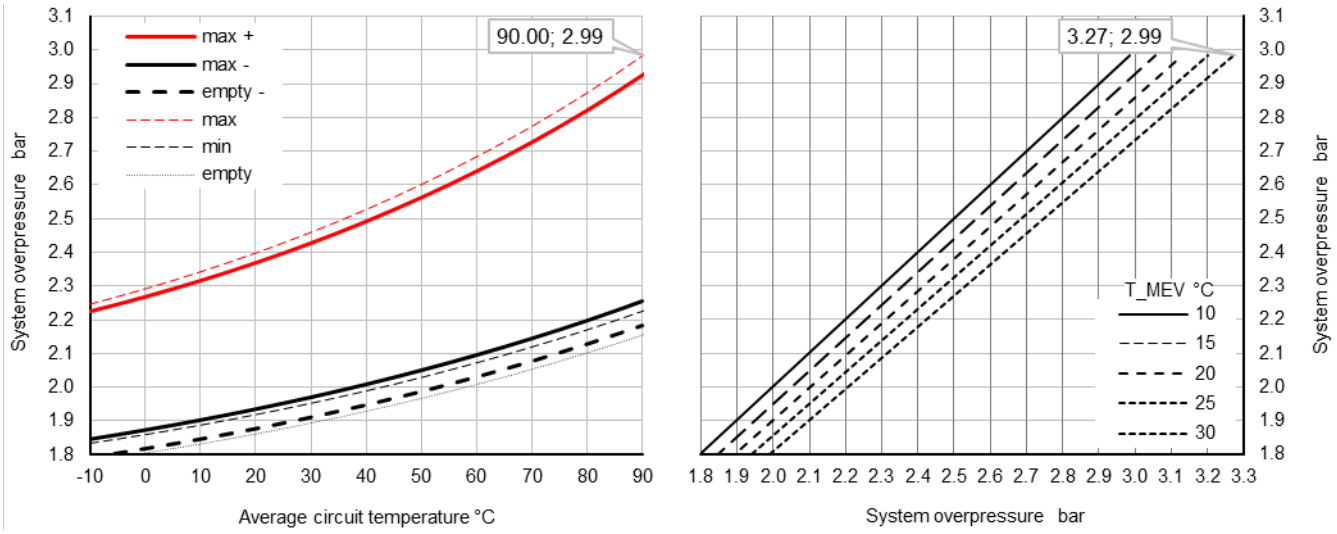

Figure 16. Left diagram: Pressure range as a function of average circuit temperature. Right diagram: Transformation to different MEV temperatures. Both diagrams are valid for the specified solar thermal circuit.

Table 6 shows minimum required and maximum permitted values, and the calculated values based on the worst-case uncertainties. The proposed method yields a larger nominal MEV volume than the method according to VDI. For solar thermal plants, one has to distinguish between the high points of

the circuit and the collector field. The pressure at the high point of the collector field in State 2 is relevant for the dimensioning, as indicated by the highlighted cells.

Table 6 Solar thermal circuit, Variant A: MEV volume, and comparison of required/permitted and calculated values.

V_N	Proposed method	L	600	VDI	500
Quantity			State 1	State 2	State 3
$V_{res,0}$	Required	L	6.0	-	-
	Calculated at $p_{0,min,lim}$	L	84.6	-	-
	Calculated at $p_{0,opt}$	L	6.0	-	-
p_H	Required, $V_{res} = 0$	bar	0.20	0.52	-
	Calculated, pump off	bar	0.68	1.05	-
	Calculated, pump on	bar	0.38	0.75	-
p_S	Required, $V_{res} = 0$	bar	0.20	0.75	-
	Calculated, pump off	bar	0.68	1.05	-
	Calculated, pump on	bar	0.38	0.75	-
p_P	Required	bar	0.50	1.20	-
	Calculated	bar	1.08	1.45	-
p_{max}	Permitted	bar	-	-	5.40
	Calculated	bar	-	-	5.40

3.4. Uncertainties of expansion volume

The expansion volume is subject to three uncertainties. First, there is the uncertainty regarding the circuit volume. This can be relatively high if detailed design documents are not available. In this case, the dimensions of the circuit components should be estimated with a generous allowance. Consequently, the MEV size is safe. This type of uncertainty can be eliminated through detailed planning. Second, neglecting the thermal expansion of the circuit material results in a systematic error. If this error is acceptable, the MEV volume is safe. Third, the uncertainty from calculating the expansion volumes based on the average temperatures, ϑ_1, and ϑ_2, rather than on the temperatures of the circuit sections and their corresponding volumes, which would be closer to reality.

When the thermal expansion of the circuit components was neglected, the permissible, filling-pressure range was narrower and located within the filling-pressure range that results from the consideration of the thermal expansion of the circuit components.

For metallic-circuit components, safety can be increased by neglecting the thermal expansion of the circuit components. If the circuit consists mainly of plastic components, for example, in floor-heating systems, the thermal expansion should be considered.

According to the standard DIN EN 13831 (2007), the actual MEV volume, excluding the diaphragm volume, can be approximately 5% smaller than the nominal volume, V_N. Therefore, a reduced volume should be used for dimensioning. Thus, the maximum, permissible-system pressure is reduced accordingly. However, the minimum, required-system pressure is not affected. The standard does neither define positive deviations from the nominal volume nor the volume of the membrane.

4. Conclusions and outlook

4.1. Purpose and advantages of the proposed method

Regardless of the method selected, MEV dimensioning is an engineering task, and only the planning engineer has knowledge of the required data. Therefore, it is the planning engineer's responsibility to provide the installer with a complete set of information on how to build, commission, and maintain a PMS. Furthermore, the information should include specifications of the pressure-gage accuracy class. The method proposed in this study was developed to achieve this goal and facilitate the tasks of both the planning engineer and the installer. The proposed dimensioning method has the following features:

1. The model allows to formally account for the following measurement uncertainties:
    a. Preset pressure
    b. System pressure.
    c. MEV temperature
    d. Average circuit temperature
2. The temperature change of the MEV is accounted for.
3. The atmospheric pressure is calculated as a function of altitude.
4. The liquid-reserve volume is explicitly defined, which enables objective assessment of the filling status of the circuit.
5. Circuit-specific diagrams enable the installer to determine the filling conditions of a circuit during commissioning and maintenance.

The consistency of the method and tool was tested with numerical examples. It has been demonstrated that pressure-measurement uncertainties must be considered. It is suggested that high-quality and accurate pressure gages be used, rather than using a larger MEV to compensate for the uncertainty of cheap gages.

Assuming that the temperature changes of the MEV are negligible, the proposed method yields the same MEV volume as the method in VDI 4708. This is an intriguing result considering that the proposed method accounts for pressure measurement uncertainties, whereas the method in VDI 4708 does not. However, in most cases, temperature changes occur and must be considered.

Compared to existing methods, the proposed method offers the following practical advantages:

- The preset and system pressure ranges are shown in the circuit-specific diagrams. This facilitates commissioning and maintenance.
- The filling status of the circuit can be reliably assessed based on pressure and temperature measurements.
- Malfunctions of hydronic circuits attributed to poorly dimensioned or inadequately maintained MEVs can be largely avoided.

Owing to these advantages, this method makes an important contribution to the energy efficiency and reliability of hydronic systems.

4.2. Need for further research

To date, no experimental studies have been conducted. From the author's viewpoint, however, it is necessary to experimentally quantify the uncertainties of the assumptions made and, if necessary, replace them with corrected assumptions. The following questions are the primary focus:

- The uncertainty in determining the mean circuit temperature should be quantified.
- Possible differences between the gas and system pressures, which could depend on the design of the vessel, elasticity of the membrane, and the volume fraction of liquid within the MEV, should be investigated by experiments on MEVs with an archetypical design.
- The temperature distribution of the vessel wall is hardly ever completely isothermal for two reasons. On the one hand, heat losses from thermal storage or boilers can result in significant temperature stratification of room air. Additionally, the temperature of the membrane can be influenced by the liquid displaced from the circuit into the MEV. Determination of the average gas temperature requires a suitable model that must be calibrated experimentally.

Supplementary Materials: A software tool was developed in Visual Basic in Excel and provided as a free open-source tool under the MIT license: https://sourceforge.net/projects/d-mev/

Funding: This study received no external funding.

Competing interests: There are no competing interests to declare.

Acknowledgements: The author would like to express his gratitude to Catherine Shultis (FHNW) for proofreading the manuscript and providing important suggestions to improve comprehensibility. Thank you Dr.-Ing. Karin Rühling (TU Dresden), and Dipl.-Ing. Christian Thesing (IMI Hydronic Engineering) for their contributions to the discussion and critical comments. This study was supported by a sabbatical grant from FHNW, University of Applied Science, Northwestern Switzerland.

5. Appendix A

Quantity	Symbol	Unit
Elevation above sea level = Reference level, i.e., bottom of the MEV	h_0	m
Height difference between highpoint of collectors and reference level	Δh_S	m
Height difference between highpoint of circuit and reference level	Δh_H	m
Height difference between pump inlet and reference level	Δh_P	m
Height difference between reference point and reference level	Δh_R	m
Atmospheric pressure	p_{Atm}	Pa
Overpressure	$\hat{p}$	Pa
Hydrostatic pressure	Δp_{st}	Pa
Pressure within the MEV in State *k*	p_k	Pa
Vapor pressure	p_v	Pa
Safety relief valve, opening pressure	p_{SV}	Pa
Safety relief valve, reseating pressure difference	Δp_{SV}	Pa
Preset pressure of the gas content within the MEV	p_0	Pa
Pressure allowance, total (VDI)	Δp_z	Pa
Minimum pressure above vapor and atmospheric pressure	$\Delta p_{z,0}$	Pa
Pressure allowance to compensate preset pressure loss	$\Delta p_{z,1}$	Pa
Pressure allowance to generate water reserve (VDI)	$\Delta p_{z,2}$	Pa
Temperature of the gas volume inside MEV in State k	T_k	K
Circuit volume without IV and MEV	V_C	m^3
Nominal MEV volume from standard series	V_N	m^3
Reserve volume, minimum required for pressure transfer	$V_{\mathrm{Res},0}$	m^3
Reserve volume, usable	V_{Res}	m^3
Reserve volume (VDI)	V_V	m^3
Displaced liquid volume between State 1 and State k	ΔV_{1-k}	m^3
Process volume	ΔV_Z	m^3
Thermal expansion coefficient of circuit materials	β	1/K
State parameter, 0 or 1, defines the location of the integration point	δ_I	-
State parameter, 0 or 1, defines the state of the pump	$\delta_{P,k}$	-
Fraction of circuit volume	γ_C	-
Fraction of MEV volume	γ_N	-
Liquid density in State k	ρ_k	kg/m^3
Average circuit temperature in State k	ϑ_k	°C
Indices		
Highpoints of circuit and solar collector field	*H, S*	
Arbitrary state between States1 and 2	*F*	
Reference point, Connection of expansion line with circuit	*R*	
Pump	*P*	
State	*k*	
States 1, 2, and 3	1, 2, 3	

6. Appendix B

Figure 17 shows the standard atmospheric pressure as a function of the altitude above sea level for various capital cities.

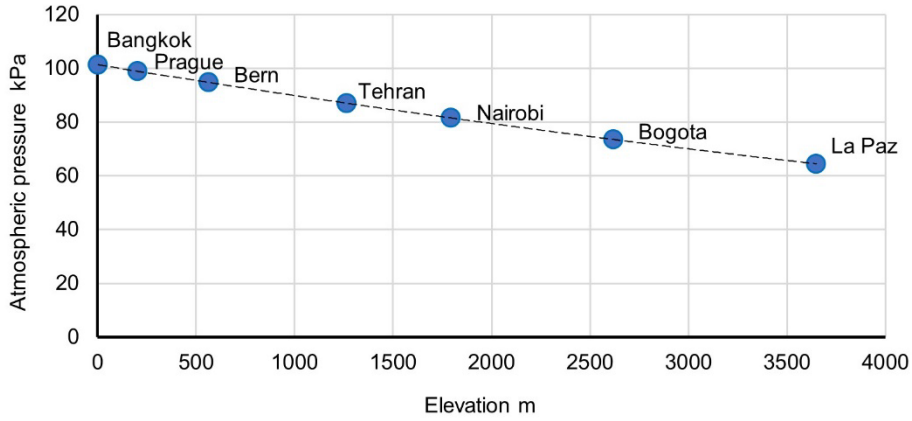

Figure 17. Standard atmospheric pressure as a function of elevation above sea level.

Figure 13 shows the densities and the vapor pressure of water and Tyfocor®LS, which is a mixture of 42% propylene glycol, 1-2% corrosion inhibitors, and water (Panitz 2021). The fluid properties were taken from VDI Heat Atlas (VDI 2013) and the datasheet of Tyfocor®LS (TYFOROP 2015) and approximated by Equations (60)–(63).

$$\rho_{\mathrm{Water}} = 1000 - 3.6066 \cdot 10^{-3}\,\vartheta - 5.4298 \cdot 10^{-3}\,\vartheta^2 + 1.2191 \cdot 10^{-5}\,\vartheta^3 \quad \mathrm{kg/m^3} \tag{62}$$

$$\rho_{\mathrm{Tyfocor\ LS}} = 1045.5 - 0.49241 \cdot \vartheta - 1.8116 \cdot 10^{-3}\,\vartheta^2 \quad \mathrm{kg/m^3} \tag{63}$$

$$p_{v,\mathrm{Water}} = 2.498 \cdot 10^{-11} \left(\vartheta + 90\right)^{6.8473} \quad \mathrm{Pa} \tag{64}$$

$$p_{v,\mathrm{Tyfocor\,LS}} = 1.516 \cdot 10^{-5} \left(\vartheta + 28\right)^{4.6446} \quad \mathrm{Pa} \tag{65}$$

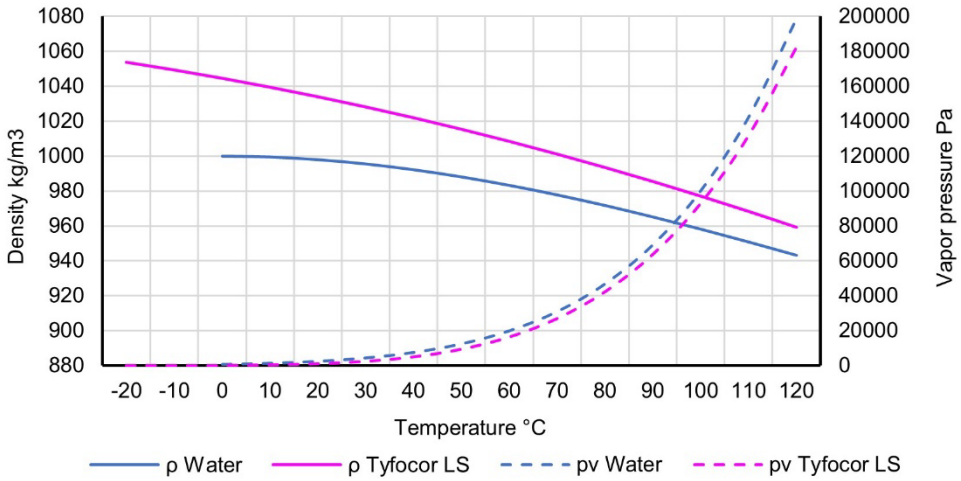

Figure 18. Density and vapor pressure of water and Tyfocor LS.

Table 7 lists the standard series of the MEV volumes used in these examples.

Table 7 Standard series of MEVs.

V_N in liters									
80	100	140	200	250	300	400	500	600	800

7. References

ASHRAE (2020) Heating, Ventilating and Air-Conditioning - Systems and Equipment. SI-Edition. American Society of Heating, Refrigerating & Air-Conditioning Engineers ASHRAE, Tullie Circle, N.E., Atlanta,

Certuse J. P. (2012) Forensic Engineering Investigation Of Hot Water Boiler And Heater Relief Valve Failures. Journal of the National Academy of Forensic Engineers 29 (1)

Chen H., Chen A., Hahn W., Riley J., Williams L., Henry R. (2018) Pressure Control Issue With TES on Large Campus Chilled Water Loop. ASHRAE journal 60 (3):68-73

Coad W. (1980) Expansion tanks. HPAC Engineering (5):85-86

Davis R. (1987) Corrosion problems in central heating systems. Anti-Corrosion Methods and Materials 34 (9):6-11

de Keizer A., Vajen K., Jordan U. (2008) Overview of Monitoring and Failure Detection Approaches for Solar Thermal Systems. In: EUROSUN, Lisbon, Portugal, 07-10 October 2008.

DIN EN 12828 (2014) Heating systems in buildings . Design for water-based heating systems. Beuth Verlag, Berlin

DIN EN 13831 (2007) Closed expansion vessels with built in diaphragm for installation in water. Beuth Verlag, Berlin

Eismann R. (2017) Thermohydraulische Dimensionierung von Solaranlagen : Theorie und Praxis der kostenoptimierenden Anlagenplanung. Springer Vieweg, Wiesbaden, ISBN: 978-3-658-07124-0, https://doi.org/10.1007/978-3-658-07125-7

Eismann R., Hummel S., Giovannetti F. (2021) A Thermal-Hydraulic Model for the Stagnation of Solar Thermal Systems with Flat-Plate Collector Arrays. Energies 14 (3):733. http://dx.doi.org/10.3390/en14030733

Gallagher M. (2022) A Multi-Lesson Hydronics War Story. ASHRAE journal 64 (1):22-26

Hausner R., Fink C., Wagner W., Riva R., Hillerns F. (2003) Entwicklung von thermischen Solarsystemen mit unproblematischem Stagnationsverhalten, Bundesministerium für Verkehr Innovation und Technologie, Wien http://www.aee-intec.at/0uploads/dateien4.pdf

Ho N. (2021) Low System Pressure Case Study: Troubleshooting Campus Chilled Water Systems. ASHRAE journal 63 (3)

Kirk C. H. (1962) Expansion tank. US3035614A, Patents US

Lockhart H., Carlson G., Grove III M. (1953) Compression tank selection for hot water heating systems. ASHVE Transactions 59:55-76

Panitz F. (2021) Löslichkeit von Gasen in Wasser-Glykol-Kreisläufen energietechnischer Anlagen. Dissertation, Technische Universität Dresden, https://doi.org/10.25368/2022.6,

Polchinski R. (2013) Avoiding System Problems When Using Expansion Tanks. ASHRAE Transactions 119 (1)

Pop O., Abrudan A., Pop I. (2015) Closed Expansion Vessel Dimensioning-Part III. ACTA TECHNICA NAPOCENSIS-Series: APPLIED MATHEMATICS, MECHANICS, and ENGINEERING 58 (1)

Scheuren J. (2008) Untersuchungen zum Stagnationsverhalten solarthermischer Kollektorfelder. Dissertation, Universität Kassel, Fachbereich Maschinenbau, https://www.uni-kassel.de/upress/online/frei/978-3-89958-430-1.volltext.frei.pdf

Stuecklin P. (1959) Expansionsgefäss für Warmwasseranlagen. CH376627 A, Schweizerisches Patentamt

SWKI (2020) HE301-01: Sicherheitstechnische Einrichtungen für Heizungsanlagen. Schweizerischer Verein von Gebäudetechnik-Ingenieuren SWKI, Urtenen-Schönbühl

Taylor S. T. (2016) The fundamentals of expansion tanks. ASHRAE journal (11):60-66

Taylor S. T. (2003) Understanding expansion tanks. ASHRAE journal 45 (3):24-30

Thomas D., Freytag J. (2009) Aeronautical tables and formulae. Neue flugtechnische Reihe vol. 1, 3rd. TFT-Verlag, Fürstenfeldbruck, 978-3-931776-07-7,

TYFOROP (2015) Technical Information: TYFOCOR LS. TYFOROP CHEMIE GmbH. https://www.tyfo.de/uploads/TI/Ti_TYFOCOR-LS_gb.pdf. Accessed 07-08-2015

VDI 4708-1 (2012) Pressure maintenance, venting, deaeration - Part 1: Pressure maintenance. Beuth Verlag, Berlin

VDI (2013) VDI-Wärmeatlas. 11. Springer-Verlag, Heidelberg, Dordrecht, London, New York, http://dx.doi.org/10.1007/978-3-642-19981-3